

# Phenomenology of Dark Matter from $A_4$ Flavor Symmetry

M. S. Boucenna,<sup>\*</sup> M. Hirsch,<sup>†</sup> S. Morisi,<sup>‡</sup> E. Peinado,<sup>§</sup> M. Taoso,<sup>¶,\*\*</sup> and J. W. F. Valle<sup>††</sup>  
*AHEP Group, Institut de Física Corpuscular – C.S.I.C./Universitat de València*  
*Edificio Institutos de Paterna, Apt 22085, E-46071 Valencia, Spain*

We investigate a model in which Dark Matter is stabilized by means of a  $Z_2$  parity that results from the same non-abelian discrete flavor symmetry which accounts for the observed pattern of neutrino mixing. In our  $A_4$  example the standard model is extended by three extra Higgs doublets and the  $Z_2$  parity emerges as a remnant of the spontaneous breaking of  $A_4$  after electroweak symmetry breaking. We perform an analysis of the parameter space of the model consistent with electroweak precision tests, collider searches and perturbativity. We determine the regions compatible with the observed relic dark matter density and we present prospects for detection in direct as well as indirect Dark Matter search experiments.

PACS numbers: 95.35.+d 11.30.Hv 14.60.-z 14.60.Pq 12.60.Fr 14.80.Cp 14.60.St 23.40.Bw

## I. INTRODUCTION

The existence of non-baryonic Dark Matter (DM) is well established by cosmological and astrophysical probes. However, despite the great experimental effort over many years, its nature still remains elusive. Elucidating the long-standing puzzle of the nature of dark matter constitutes one of the most important challenges of modern cosmology and particle physics.

The various observations and experiments, however, constrain some of its properties [1, 2]. Among the most important requirements a DM candidate is required to satisfy are neutrality, stability over cosmological time scales, and agreement with the observed relic density. While the neutrality of the particle is usually easy to accommodate in models, its stability in general is assumed in an *ad-hoc* fashion. From a particle physics point of view, the stability suggests the existence of a symmetry that forbids the couplings that would otherwise induce the decay. Typically, the most common way to stabilize the DM particle is to invoke a  $Z_2$  parity, an example of which is R parity in supersymmetry.

It would certainly be more appealing to motivate such a symmetry from a top-down perspective. Different mechanisms have been suggested to achieve this [3], for instance using  $U(1)$  gauge symmetries [4–6] to get for example R-parity in the MSSM from a  $U(1)_{B-L}$  [7] symmetry, global symmetries, accidental symmetries [8] or custodial symmetry.

A new mechanism of stabilizing the DM has been recently proposed in Ref. [9] in which DM stability originates from the flavor structure of the standard model. Indeed the same discrete flavor symmetry which explains the pattern of neutrino mixing [10] can also stabilize the dark matter <sup>1</sup>. This opens an attractive link between neutrino physics and DM <sup>2</sup>; two sectors that show a clear need for physics beyond the Standard Model.

---

<sup>¶</sup> Multidark fellow

<sup>\*</sup>Electronic address: boucenna@ific.uv.es

<sup>†</sup>Electronic address: mahirsch@ific.uv.es

<sup>‡</sup>Electronic address: morisi@ific.uv.es

<sup>§</sup>Electronic address: epeinado@ific.uv.es

<sup>\*\*</sup>Electronic address: taoso@ific.uv.es

<sup>††</sup>Electronic address: valle@ific.uv.es

<sup>1</sup> Models based on non-Abelian discrete symmetries but with a decaying dark matter candidate can be found for example in Ref.[11].

<sup>2</sup> Other mechanisms of relating DM and neutrinos include the majoron DM [12–14].

The model proposed in Ref. [9] is based on an  $A_4$  symmetry extending the Higgs sector of the SM with three scalar doublets. After electroweak symmetry breaking two of the scalars of the model acquire vacuum expectation values (vev) which spontaneously break  $A_4$  leaving a residual  $Z_2$ . The lightest  $Z_2$  neutral odd scalar is then automatically stable and will be our DM candidate.

On the other hand, the fermionic sector is extended by four right handed neutrinos which are singlets of  $SU(3) \times SU(2) \times U(1)$ . Light neutrino masses are generated via a type I see-saw mechanism [15–19], obey an inverted hierarchy with  $m_{\nu 3} = 0$  and vanishing reactor neutrino angle <sup>3</sup>. For pioneer studies on the use of  $A_4$  for neutrino physics see [21].

We study the regions in parameter space of the model where the correct dark matter relic density is reproduced and the constraints from accelerators are fulfilled. We then consider the prospects for direct dark matter detection in underground experiments. We show that the model can potentially explain the DAMA annual modulation data [22, 23] as well as the excess recently found in the COGENT experiment [24]. We show that present upper limits on the spin independent DM scattering cross section off nucleons can already severely constrain the parameter space of the model. Indirect dark matter searches through astrophysical observations are not currently probing the model apart from some small regions of the parameter space where the dark matter annihilation cross section is enhanced via a Breit-Wigner resonance.

The paper is organized as follows: in Sec.II we present the model, in Sec. III the constraints from collider data are reviewed and in Section IV we study the viable regions of the parameter space. In Sec. V and VI we sketch the prospects for direct and indirect dark matter detection. Finally, we summarize our conclusions in Sec. VII.

## II. THE MODEL

We now provide a concrete realization of dark matter based upon the  $A_4$  flavor symmetry adopting the simple type-I seesaw framewok [15–19]. In order to be phenomenologically viable, the model should account not only for the mixing angles describing the observed pattern of neutrino oscillations [10] but also for the two independent square mass splittings characterizing the “solar” and “atmospheric” sectors. These points were taken into account in the model proposed in [9] which we now adopt, and consider its phenomenological features in more detail. The matter fields are assigned to irreducible representations of the group of even permutations of four objects  $A_4$  [9], which is isomorphic to the symmetry group of the tetrahedron, for more details see Appendix A. The standard model Higgs doublet  $H$  is assigned to a singlet representation, while the three additional Higgs doublets  $\eta = (\eta_1, \eta_2, \eta_3)$  transform as an  $A_4$  triplet, namely  $\eta \sim 3$ . The model has in total four Higgs doublets, implying the existence of four CP even neutral scalars, three physical pseudoscalars, and three physical charged scalar bosons.

In the fermion sector we have four right-handed neutrinos; three transforming as an  $A_4$  triplet  $N_T = (N_1, N_2, N_3)$ , and one singlet  $N_4$ . Quarks are assigned trivially as  $A_4$  singlets, as a result of which there are no predictions on their mixing matrix, as it is difficult to reconcile quarks with the neutrino sector <sup>4</sup>.

The lepton and Higgs assignments are summarized in table I.

	$L_e$	$L_\mu$	$L_\tau$	$l_e^c$	$l_\mu^c$	$l_\tau^c$	$N_T$	$N_4$	$\hat{H}$	$\eta$
$SU(2)$	2	2	2	1	1	1	1	1	2	2
$A_4$	1	1'	1''	1	1''	1'	3	1	1	3

TABLE I: Summary of the relevant quantum numbers

<sup>3</sup> For a similar realisation see [20].

<sup>4</sup> The formulation of a full theory of flavour is beyond the scope of this work and will be left for the future.

The resulting leptonic Yukawa Lagrangian is:

$$\begin{aligned} \mathcal{L} = & y_e L_e l_e^c \hat{H} + y_\mu L_\mu l_\mu^c \hat{H} + y_\tau L_\tau l_\tau^c \hat{H} + \\ & + y_1' L_e (N_T \eta)_1 + y_2' L_\mu (N_T \eta)_{1'} + y_3' L_\tau (N_T \eta)_{1'} + \\ & + y_4' L_e N_4 \hat{H} + M_1 N_T N_T + M_2 N_4 N_4 + \text{h.c.} \end{aligned} \quad (1)$$

This way the field  $\hat{H}$  is responsible for quark and charged lepton masses, the latter automatically diagonal. The scalar potential is:

$$\begin{aligned} V = & \mu_\eta^2 \eta^\dagger \eta + \mu_{\hat{H}}^2 \hat{H}^\dagger \hat{H} + \lambda_1 [\hat{H}^\dagger \hat{H}]_1^2 + \lambda_2 [\eta^\dagger \eta]_1^2 + \lambda_3 [\eta^\dagger \eta]_{1'} [\eta^\dagger \eta]_{1''} \\ & + \lambda_4 [\eta^\dagger \eta]_{1'} [\eta \eta]_{1''} + \lambda_{4'} [\eta^\dagger \eta]_{1''} [\eta \eta]_{1'} + \lambda_5 [\eta^\dagger \eta]_1 [\eta \eta]_1 + \lambda_6 ([\eta^\dagger \eta]_{3_1} [\eta^\dagger \eta]_{3_1} + \text{h.c.}) \\ & + \lambda_7 [\eta^\dagger \eta]_{3_1} [\eta^\dagger \eta]_{3_2} + \lambda_8 [\eta^\dagger \eta]_{3_1} [\eta \eta]_{3_2} + \lambda_9 [\eta^\dagger \eta]_{1'} [\hat{H}^\dagger \hat{H}] + \lambda_{10} [\eta^\dagger \hat{H}]_{3_1} [\hat{H}^\dagger \eta]_{3_1} \\ & + \lambda_{11} ([\eta^\dagger \eta]_1 \hat{H} \hat{H} + \text{h.c.}) + \lambda_{12} ([\eta^\dagger \eta]_{3_1} [\eta \hat{H}]_{3_1} + \text{h.c.}) + \lambda_{13} ([\eta^\dagger \eta]_{3_2} [\eta \hat{H}]_{3_1} + \text{h.c.}) + \lambda_{14} ([\eta^\dagger \eta]_{3_1} \eta^\dagger \hat{H} + \text{h.c.}) \\ & + \lambda_{15} ([\eta^\dagger \eta]_{3_2} \eta^\dagger \hat{H} + \text{h.c.}) \end{aligned} \quad (2)$$

where  $[\dots]_{3_{1,2}}$  is the product of two triplets contracted into one of the two triplet representations of  $A_4$ , see eq. (A4), and  $[\dots]_{1,1',1''}$  is the product of two triplets contracted into a singlet representation of  $A_4$ . In what follows we assume, for simplicity, CP conservation, so that all the couplings in the potential are real. For convenience we also assume  $\lambda_4 = \lambda_4'$  in order to have manifest conservation of CP in our chosen  $A_4$  basis<sup>5</sup>.

The minimization of the scalar potential results in :

$$\langle H^0 \rangle = v_H \neq 0, \quad \langle \eta_1^0 \rangle = v_\eta \neq 0, \quad \langle \eta_{2,3}^0 \rangle = 0, \quad (3)$$

where all vevs are real. This vev alignment breaks the group  $A_4$  to its subgroup  $Z_2$  responsible for the stability of the DM as well as for the neutrino phenomenology [9]. In Appendix B we comment on a possible embedding of the model into the grand unified group  $SU(5)$ .

#### *The stability of the DM*

Since there are no couplings with charged fermions nor quarks because of the  $A_4$  symmetry, the only Yukawa interactions of the lightest neutral component of  $\eta_{2,3}$  are with the heavy  $SU(3) \times SU(2) \times U(1)$  singlet right-handed neutrinos. This state is charged under the  $Z_2$  parity that survives after the spontaneous breaking of the flavor symmetry. One finds that, as a consequence of this  $Z_2$  symmetry, the mass matrix for the neutral scalars is block-diagonal, see eq. (C8), so that the lightest neutral component of  $\eta_{2,3}$  is not mixed with the two Higgs scalars that take vev,  $H$  and  $\eta_1$ . Thus quartic couplings will not induce decays for this DM candidate which is therefore stable and constitutes our DM candidate.

We now show the origin of such a parity symmetry.

As explained in Appendix A, the group  $A_4$ , has two generators:  $S$ , and  $T$ , that satisfy the relations  $S^2 = T^3 = (ST)^3 = I$ . In the three dimensional basis  $S$  is given by

$$S = \begin{pmatrix} 1 & 0 & 0 \\ 0 & -1 & 0 \\ 0 & 0 & -1 \end{pmatrix}. \quad (4)$$

$S$  is the generator of the  $Z_2$  subgroup of  $A_4$ . The alignment  $\langle \eta \rangle \sim (1, 0, 0)$  breaks spontaneously  $A_4$  to  $Z_2$  since  $(1, 0, 0)$  is manifestly invariant under the  $S$  generator:

$$S \langle \eta \rangle = \langle \eta \rangle. \quad (5)$$

---

<sup>5</sup> To see this, consider for instance the coupling  $(\omega \lambda_4 + \omega^2 \lambda_4') (\eta_1^\dagger \eta_2)^2 + \text{h.c.}$  arising from the terms proportional to  $\lambda_4$  and  $\lambda_4'$  in eq. (2). Since  $\omega + \omega^2 = -1$  this coupling is real if and only if  $\lambda_4 = \lambda_4'$ .

For a generic triplet irreducible representation of  $A_4$ ,  $\Psi = (a_1, a_2, a_3)^T$ , we have:

$$S\Psi = \begin{pmatrix} 1 & 0 & 0 \\ 0 & -1 & 0 \\ 0 & 0 & -1 \end{pmatrix} \begin{pmatrix} a_1 \\ a_2 \\ a_3 \end{pmatrix} = \begin{pmatrix} a_1 \\ -a_2 \\ -a_3 \end{pmatrix}. \quad (6)$$

The  $Z_2$  residual symmetry is defined as

$$\begin{aligned} N_1 &\rightarrow +N_1, & \eta_1 &\rightarrow +\eta_1, \\ N_2 &\rightarrow -N_2, & \eta_2 &\rightarrow -\eta_2, \\ N_3 &\rightarrow -N_3, & \eta_3 &\rightarrow -\eta_3, \end{aligned} \quad (7)$$

and the rest of the matter fields are  $Z_2$  even, because the singlet representation transforms trivially under  $S$ , see Appendix A. This is the residual symmetry which is responsible for the stability of our DM candidate.

### Neutrino phenomenology

Here we summarize the main results obtained in Ref.[9] concerning the neutrino phenomenology. The model contains four heavy right-handed neutrinos so it is a special case, called (3,4), of the general type-I seesaw mechanism [19]. After electroweak symmetry breaking, it is characterized by Dirac and Majorana mass-matrix:

$$m_D = \begin{pmatrix} x_1 & 0 & 0 & x_4 \\ x_2 & 0 & 0 & 0 \\ x_3 & 0 & 0 & 0 \end{pmatrix}, \quad M_R = \begin{pmatrix} M_1 & 0 & 0 & 0 \\ 0 & M_1 & 0 & 0 \\ 0 & 0 & M_1 & 0 \\ 0 & 0 & 0 & M_2 \end{pmatrix}. \quad (8)$$

where  $x_1, x_2, x_3$  and  $x_4$  are respectively proportional to  $y_1^\nu, y_2^\nu, y_3^\nu$  and  $y_4^\nu$  of eq.(1) and are of the order of the electroweak scale, while  $M_{1,2}$  are assumed close to the unification scale. Light neutrinos get Majorana masses by means of the type-I seesaw relation and the light-neutrinos mass matrix has the form:

$$m_\nu = -m_{D_{3 \times 4}} M_{R_{4 \times 4}}^{-1} m_{D_{3 \times 4}}^T \equiv \begin{pmatrix} y^2 & ab & ac \\ ab & b^2 & bc \\ ac & bc & c^2 \end{pmatrix}. \quad (9)$$

This texture of the light neutrino mass matrix has a null eigenvalue  $m_3 = 0$  corresponding to the eigenvector  $(0, -b/c, 1)^T$ ,<sup>6</sup> implying a vanishing reactor mixing angle  $\theta_{13} = 0$  and inverse hierarchy. The atmospheric angle, the solar angle and the two square mass differences can be fitted. The model implies a neutrinoless double beta decay effective mass parameter in the range 0.03 to 0.05 eV at  $3\sigma$ , within reach of upcoming experiments.

### Notation

After electroweak symmetry breaking and the minimization of the potential we can write:

$$\begin{aligned} \hat{H} &= \begin{pmatrix} H_0'^+ \\ (v_H + H_0' + iA_0')/\sqrt{2} \end{pmatrix}, & \eta_1 &= \begin{pmatrix} H_1'^+ \\ (v_\eta + H_1' + iA_1')/\sqrt{2} \end{pmatrix}, \\ \eta_2 &= \begin{pmatrix} H_2'^+ \\ (H_2' + iA_2')/\sqrt{2} \end{pmatrix}, & \eta_3 &= \begin{pmatrix} H_3'^+ \\ (H_3' + iA_3')/\sqrt{2} \end{pmatrix}. \end{aligned} \quad (10)$$

---

<sup>6</sup> Note that if we were to stick to the minimal (3,3)-type-I seesaw scheme, with just 3 SU(2) singlet states, one would find a projective nature of the effective tree-level light neutrino mass matrix with two zero eigenvalues, hence phenomenologically inconsistent. That is why we adopted the (3,4) scheme.

The structure of the neutral and charged scalar mass matrices follows from the exact  $Z_2$  symmetry, which forbids mixings between particles with different  $Z_2$  parities and from CP conservation. As a result the charged and neutral scalar mass matrices decompose into two-by-two mass matrices which, after diagonalization, give the scalar mass spectrum of the model. In what follows, unprimed particles denote mass eigenstates. We refer to Appendix C for details about the mass matrices and for a complete description of the mass spectrum. The  $Z_2$ -odd sector contains two real CP even scalars,  $H_2$  and  $H_3$ , two real CP odd scalars,  $A_2$  and  $A_3$ , and four charged scalars,  $H_2^\pm$  and  $H_3^\pm$ . The  $Z_2$  even scalars consist of two real CP even scalars  $H$  and  $H_0$ , that we generically call 'Higgses', a pseudoscalar  $A_0$  and two charged scalars  $H_0^\pm$ . The masses of the  $W^\pm$  and  $Z$  gauge bosons impose the relation  $v_H^2 + v_\eta^2 = v^2$  where  $v$  stands for the standard model value of the vev. We call  $\tan\beta$  the ratio of the two vevs:  $\tan\beta = v_H/v_\eta$ .

The DM candidate of the model corresponds to the lightest  $Z_2$ -odd neutral spin zero particle which, for the sake of definiteness, we take as the CP-even state  $H_2$ . We remind that the parameters of the model relevant for the DM phenomenology are the 15 couplings of the scalar potential,  $\lambda_i$ , and the ratio of the vacuum expectation values  $\tan\beta = v_H/v_\eta$ . Indeed the minimization of the scalar potential and electroweak symmetry breaking allow to recast the mass parameters  $\mu_H$  and  $\mu_\eta$  in terms of the couplings  $\lambda_i$  and  $\tan\beta$ . Note that the couplings and the Majorana mass parameters in Eq. Ref.1 determine the neutrino mass matrix, they are not relevant for the dark matter phenomenology. Before moving to the calculation of its relic abundance in the next section we consider the phenomenological constraints on the parameter space of the model.

### III. PHENOMENOLOGICAL CONSTRAINTS

In order to find the viable regions in parameter space where to perform our study of dark matter, we must impose the following constraints to the model :

- *Electroweak precision tests*

It is well-known that the oblique parameters  $S, T, U$  provide stringent constraints on theories beyond the Standard Model [25]. Concerning the  $S$  and  $U$  parameters, these receive negligible contributions from the scalars of the model [26, 27], hence we focus on the  $T$  parameter. We compute the effect on  $T$  induced by the scalars following [28] and we impose the bounds from electroweak measurements [29]:

$$-0.08 \leq T \leq 0.14.$$

While this bound favors a light Standard Model Higgs boson, large Higgs masses are possible in the presence of new physics, such as our multi-Higgs-doublet model. Indeed, a negative deviation of the electroweak  $T$  parameter induced by a heavy Higgs can be compensated by a positive  $\Delta T$  produced by new scalar particles of the model, so one can raise the Higgs mass up to  $\sim 600$  GeV or so (see below) <sup>7</sup>.

We have explicitly verified that we can choose the mass spectrum of the model in such a way that this constraint is always respected. We refer to Appendix D for more detail.

- *Collider bounds*

Searches for supersymmetric particles at LEP place a lower bound on the chargino mass of  $\sim 100$  GeV. To be conservative we apply this constraint also to the masses of the charged scalars of our model, even if slightly lower masses, 70 – 90 GeV, might still be consistent with LEP data[30].

The bounds imposed by LEP II on the masses of the neutral scalars in our model are similar to those constraining the Inert Doublet Model, given in Ref.[31]. This analysis applies directly to the  $Z_2$ -odd scalar sector of our model of particular interest for DM phenomenology, as it constrains the mass difference between  $H_2$  and  $A_2$ . The excluded region that we adopt is taken from Fig.7 of Ref.[31].

---

<sup>7</sup> A similar situation holds, for instance, in the Inert Doublet Model [27].

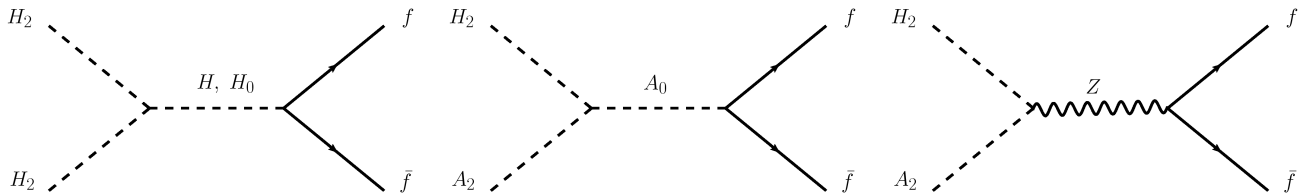


FIG. 1: Left: Tree level Feynman diagrams for the  $H_2$  annihilation into fermions. Center and right: diagrams for  $H_2$  co-annihilation with the pseudoscalar  $A_2$  into fermions.

The masses of the  $Z_2$  even neutral scalars are also constrained by LEP searches. Although a precise bound requires a detailed analysis of the even sector, we just impose a lower limit on these masses of 114 GeV, which is approximatively the LEP limit on the SM higgs mass.

We remark that lepton flavor violating processes are suppressed by the large right-handed neutrino scale.

- *Perturbativity and vacuum stability*

The requirement of perturbativity imposes the following bounds on the Yukawa couplings of the model and  $\tan\beta$  :

$$\lambda_i \lesssim \sqrt{4\pi} \quad i=1,\dots,15,$$

$$\tan\beta > 0.5$$

this leads to an upper bound on the masses of the scalars at  $\sim 600$  GeV <sup>8</sup> The constraint on  $\tan\beta$  is necessary in order to preserve a perturbative top-Yukawa coupling.

Finally we must impose the stability of the vacuum. The conditions ensuring that the potential is bounded from below are:

$$\lambda_1 > 0, \quad \lambda_2 + \lambda_3 + 2\lambda_4 + \lambda_5 > 0,$$

$$\lambda_1 + 3(\lambda_2 + \lambda_3 + 2\lambda_4 + \lambda_5) + 3(\lambda_9 + Min1) + 3(2\lambda_2 - \lambda_3 + \lambda_8 + Min2) - 6Q > 0,$$

where

$$Min1 = Min(\lambda_{10} - 2|\lambda_{11}|, 0),$$

$$Min2 = Min(\lambda_7 - 2|\lambda_4 - \lambda_5 - \lambda_6|, 0),$$

$$Q = |\lambda_{12}| + |\lambda_{13}| + |\lambda_{14}| + |\lambda_{15}|.$$

#### IV. RELIC DENSITY

---

<sup>8</sup> Note that this bound would not apply to the Inert Higgs Doublet model, which would potentially allow heavier dark matter masses.

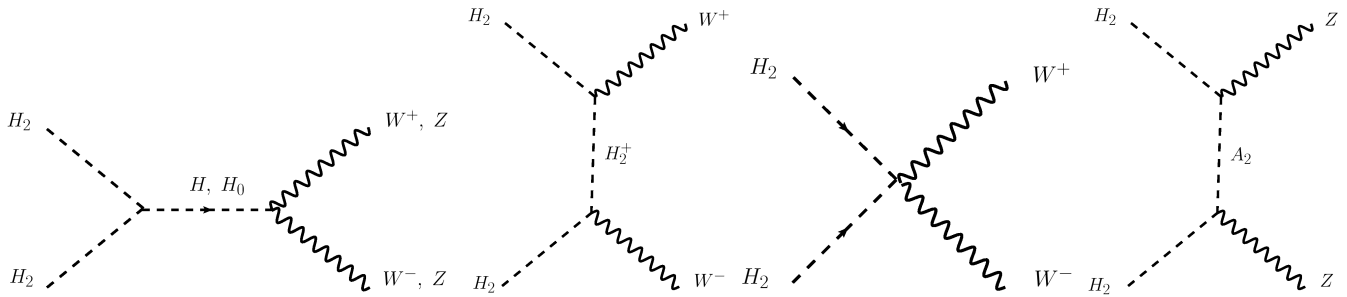


FIG. 2: Tree level Feynman diagrams for the  $H_2$  annihilation into  $W^\pm$  and  $Z Z$ .

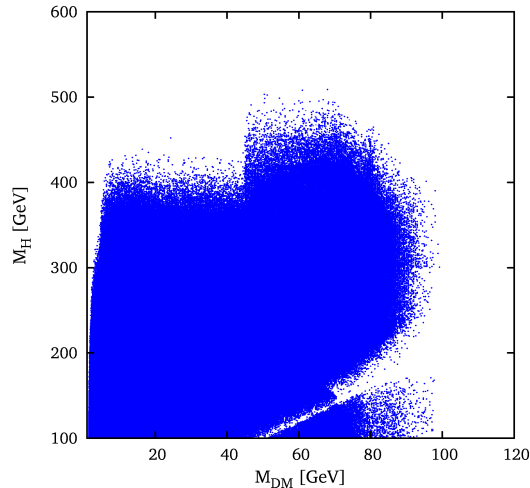


FIG. 3: Regions in the plane DM mass ( $M_{DM}$ ) - lightest Higgs boson  $M_H$  allowed by collider constraints and leading to a DM relic abundance compatible with WMAP measurements.

The thermal relic abundance of  $H_2$  is controlled by its annihilation cross section into SM particles. In Fig.1 and Fig.2 we show the Feynman diagrams for the most relevant processes. In order to study the viable regions of the model we perform a random scan over the 16-dimensional parameter space ( $\lambda_i$  and  $\tan\beta$ ) and compute the dark matter relic abundance using the micrOMEGAs package[32, 33]. Using the mass relations in equations C12 we can trade some of the couplings  $\lambda_i$  for the scalar masses. This system of 10 linear equations allows us to trade only 8 of the  $\lambda_i$ . Indeed, the texture of the mass matrix of the  $Z_2$  odd sector imposes the following constraints on the squared mass differences:  $M_{H_2}^2 - M_{H_3}^2 = 3(M_{A_2}^2 - M_{A_3}^2) = 3(M_{H_2^\pm}^2 - M_{H_3^\pm}^2)$ . We linearly sample on the 8 independent masses in such a way to fulfill the collider constraints discussed in Sec.III. The remaining 7 free  $\lambda_i$  and  $\cos\beta$  are linearly sampled inside their allowed ranges, specified in Sec.III. Then, we select those choices which satisfy the perturbativity constraints for all the 15  $\lambda_i$ , the vacuum stability bounds and for which the electroweak precision tests are satisfied. Finally, we choose only those models which provide a relic abundance consistent with the WMAP measurements:

$$0.09 \leq \Omega h^2 \leq 0.13.$$

In Fig. 3 we show the regions with a correct relic abundance in the plane DM mass ( $M_{DM}$ ) and the lightest Higgs boson mass  $M_H$ . For dark matter masses well below the  $W^\pm$  threshold, dark matter annihilations into fermions are driven by the s-channel exchange of the Higgs scalars of the model, as shown in Fig. 1.

For  $M_H \lesssim 400$  GeV the annihilation cross-sections are large enough to obtain the correct relic density for all DM masses up to the  $W^\pm$  threshold. At larger Higgs boson masses, annihilations into light fermions are suppressed so that the relic abundance is typically too large unless efficient co-annihilations with the pseudoscalar  $A_2$  or with  $H_2^\pm$  occur. These processes, shown in Fig.1 for  $A_2$ , take place only for small mass splittings between  $H_2$  and  $A_2$  or  $H_2^\pm$ .

Note that the possibility to co-annihilate with the charged scalar is ruled out, since LEP data requires  $M_{H_2}^\pm \gtrsim 100$  GeV. There is, however, a narrow window still allowed by LEP II limits on the  $A_2$ - $H_2$  plane [31] where arbitrarily small mass splitting can exist between  $H_2$  and  $A_2$  for  $M_{DM} \gtrsim 40$  GeV. For lighter dark matter particles, strong co-annihilations can not be reconciled with LEP II constraints as these require  $M_{A_2} \gtrsim 100$  GeV [31]. We can therefore exclude by cosmological observations the parameter region corresponding to (simultaneously)  $M_{DM} \lesssim 40$  GeV and  $M_H \gtrsim 400$  GeV, because the DM would be overabundant. This is clearly seen in Fig. 3. In contrast, the absence of points on the strip corresponding to the line  $M_{DM} \sim M_H/2$  is associated to the presence of the  $H$  resonance, which would enhance the DM annihilation cross section giving a too small Dark Matter abundance.

For dark matter masses larger than  $M_W$ , unless the dark matter candidate is very heavy  $M_{DM} \gtrsim 500$  GeV, the annihilation cross section into gauge bosons is typically too large so that  $H_2$  can only be a subdominant component of the dark matter budget of the Universe. However, for certain combinations of masses and parameters, the annihilations into gauge bosons may be suppressed by a cancellation between the Feynman diagrams (Fig. 2), leading to an acceptable relic density. Indeed, this happens for some points in Fig. 3<sup>9</sup>. Ref. [34] shows that these processes allow for dark matter masses up to 160 GeV, just below the threshold for annihilations into top pairs. In our scan, the viable region of the parameter space extends only up to  $M_{DM} \sim 100$  GeV. Solutions at higher masses cannot be excluded, though their scrutiny is rather involved due to the large number of parameters of the model.

We now turn to the region  $M_{DM} \sim 500$  GeV. As noted in [9], a scalar dark matter candidate annihilating into massive vector bosons inherits the correct relic abundance for this value of the mass if all other annihilation processes are absent. This scenario could be realised in our model by tuning the Yukawa couplings in order to suppress the dark matter annihilation into Higgs scalars and fermions. However, since the dark matter mass arises entirely from the electroweak symmetry breaking sector, high dark matter masses tend also to require large scalar couplings. This argument suggests that solutions with a heavy dark matter candidate and small couplings with the other scalars would be rather fine-tuned and we do not consider this possibility any further<sup>10</sup>. In the next two sections we study the prospects for direct and indirect dark matter detection.

## V. DIRECT DETECTION

Dark Matter can be searched for in underground detectors looking for nuclear recoils induced by dark matter scattering against the target material. The scalar dark matter candidate we are considering couples to quarks via Higgs boson exchange, leading therefore to pure spin independent (SI) interactions with the nucleons. In the left panel of Fig. 4 we show the SI scattering cross section off proton for the models with a correct dark matter abundance. We note that a large region of the parameter space is ruled out by the constraints imposed by current dark matter direct detection experiments.

A positive signal of dark matter detection has been claimed by the DAMA collaboration [23]. DAMA has reported a high statistical evidence for annual modulation of the event rate over 13 year cycles [22, 23]. These results have prompted many attempts to interpret the data in terms of dark matter interactions with nuclei. Assuming an elastic WIMP interactions off nuclei and for "standard" astrophysical assumption on the local DM density and velocity distribution, the DAMA signal is in conflict with the null results reported by other experiments [37, 44, 45]. However astrophysical inputs are subject to large uncertainties (see e.g. [46–48]) and, moreover, the detector response is not completely known (for example the role of channelling is still under debate [49]). We also note that there exist alternative particle physics scenarios where a compatibility between the DAMA signal and the results of other experiments can be obtained, e.g. [50–52].

<sup>9</sup> For the Inert Doublet model, these cancellations have been noted in [31] and have been recently studied in detail in [34].

<sup>10</sup> Note also that in the range  $\sim 60$  GeV- $M_W$ , annihilations into three body final states may play a role, as shown for the Inert Doublet model in [35].



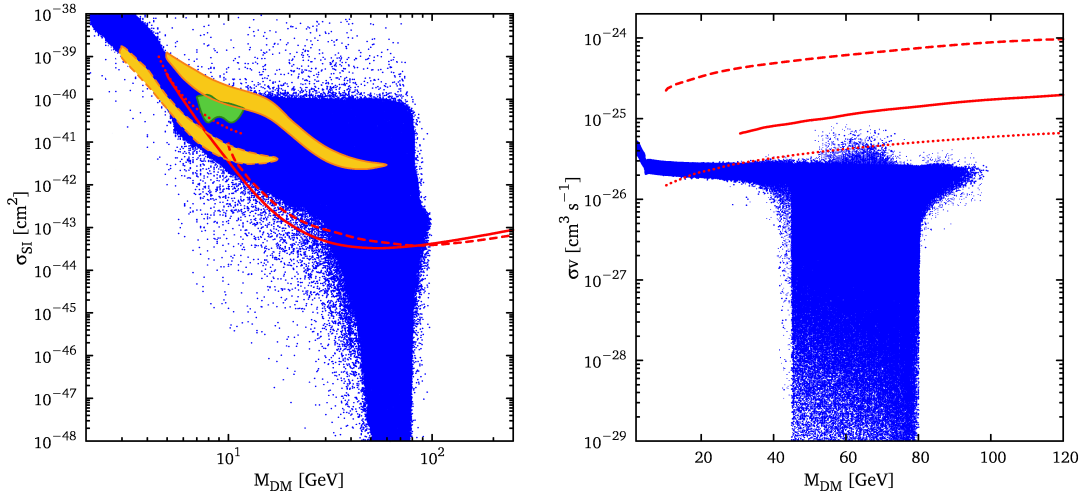


FIG. 4: Left plot: Spin-independent DM scattering cross section off-protons as a function of the dark matter mass. The orange regions delimited by the dashed (solid) line show the DAMA/LIBRA annual modulation regions including (neglecting) the channeling effect [36]. The green region corresponds to the COGENT data [37]. Dashed and dotted red lines correspond to the upper bound from CDMS (respectively from [38] and [39]). XENON100 bounds [40] are shown as a solid red line. Right plot: annihilation cross section times velocity as a function of the dark matter mass. The solid and dashed red lines show respectively the upper bound inferred by Fermi-LAT observations of the Draco dwarf galaxy [41] and FERMI-LAT measurements of the isotropic diffuse gamma-ray emission [42]. Projected 5 years sensitivity from measurements of the isotropic diffuse gamma-ray emission are shown as a dotted red line [43].

Recently, a hint of a possible signal from dark matter has been reported by the COGENT experiment [24]. In Fig.4 we show the combination of SI scattering cross section and DM masses which can fit the DAMA and COGENT results. An excess of events over the expected background has also been found by the CDMS experiment [38], although with a low statistical significance and by CRESST [53], even if these results are still preliminary. Interestingly, all these possible signals point to the same region of the parameter space, favoring low dark matter masses  $M_{DM} \lesssim 15$  GeV [36, 37, 44, 54]. As seen in Fig.4, these possible hints of dark matter detection can be accommodated within our model.

Current upper bounds severely challenge a possible interpretation of the aforementioned anomalies in terms of dark matter SI interactions. Indeed, as shown in Fig.4, the bulk of the COGENT and DAMA regions are excluded by the constraints inferred by XENON100 [40] and CDMS [38, 39]. Still, experimental uncertainties may significantly affect the upper limits obtained by direct detection experiments, especially for low mass WIMPs (see [37, 54, 55]). For this reason a possible dark matter spin-independent interpretation of the excess, even if disfavored, cannot be excluded at present.

## VI. INDIRECT DETECTION

Dark Matter indirect detection experiments look for signatures of DM annihilation into photons, neutrinos and (anti-) matter fluxes. The expected DM signals depend on the astrophysical details related to the DM density distribution in the region of observation. Particle physics enters in the determination of the DM mass, annihilation cross section  $\sigma v$  and the rates into various annihilation channels. In Fig. 4 we show  $\langle\sigma v\rangle$  at small velocity, relevant for DM annihilations inside our galaxy, as a function of  $M_{DM}$ . For  $M_{DM} \lesssim 40$  GeV  $\langle\sigma v\rangle$  remains close to the thermal value at freeze-out,  $3 \times 10^{-26}$  cm<sup>3</sup>s<sup>-1</sup>, as expected for the s-wave DM annihilation into light fermions. At larger DM masses, the presence of co-annihilations allows for much smaller values of  $\langle\sigma v\rangle$ . The solutions at  $\langle\sigma v\rangle \sim 10^{-25}$  cm<sup>3</sup>s<sup>-1</sup> correspond to DM masses just below the Higgs resonance. In this case the annihilation cross section at small velocities is boosted with respect to its values at the DM freeze-out. This behaviour of  $\langle\sigma v\rangle$  close to a narrow Breit-Wigner resonance has been recently widely exploited in order to boost the annihilation signal so to explain the cosmic-rays

anomalies reported by the PAMELA collaboration [56–59].

In order to sketch the prospects for indirect DM detection we show in Fig. 4 the constraints on  $\langle\sigma v\rangle$  imposed by the Fermi-LAT observations of the Draco dwarf spheroidal galaxy [41] and the Fermi-LAT measurements of the isotropic diffuse gamma-ray emission [42]. We caution that these upper bounds have been computed assuming DM annihilations into  $b\bar{b}$ , therefore they would directly apply only for parameter choices in our model where this annihilation channel is dominant. Still, this happens in large part of the parameter space, and in particular at low dark matter masses, where the Fermi-LAT constraints are close to the predictions of the model. For a comparison of these bounds with those obtained for different annihilation channels we refer the reader to the original references. Further constraints for different targets of observations are obtained in Ref. [60–64].

One sees from Fig. 4 that current bounds are not yet able to significantly constrain the model. However, the Fermi-LAT sensitivity is expected to improve considerably with larger statistics and for different targets of observations, see e.g. [43, 63–65]). For example, in Fig. 4 we show the forecasted 5 years FERMI-LAT sensitivities from the isotropic diffuse gamma-ray emission [43]. Fermi-LAT measurements should be able to test the model for low dark matter masses.

## VII. CONCLUSIONS AND DISCUSSION

We have studied a model where the stability of the dark matter particle arises from a flavor symmetry. The  $A_4$  non-abelian discrete group accounts both for the observed pattern of neutrino mixing as well as for DM stability. We have analysed the constraints that follow from electroweak precision tests, collider searches and perturbativity. Relic dark matter density constraints exclude the region of the parameter space where simultaneously  $M_{DM} \lesssim 40$  GeV and  $M_H \gtrsim 400$  GeV because of the resulting over-abundance of dark matter. We have also analysed the prospects for direct and indirect dark matter detection and found that, although the former already excludes a large region in parameter space, we cannot constrain the mass of the DM candidate. In contrast, indirect DM detection is not yet sensitive enough to probe our predictions. However, forecasted sensitivities indicate that Fermi-LAT should start probing them in the near future.

All of the above relies mainly on the properties of the scalar sector responsible for the breaking of the gauge and flavour symmetry. A basic idea of our approach is to link the origin of dark matter to the origin of neutrino mass and the understanding of the pattern of neutrino mixing, two of the most outstanding challenges in particle physics today. At this level one may ask what are the possible tests of this idea in the neutrino sector. Within the simplest scheme described in Ref. [9] one finds an inverted neutrino mass hierarchy, hence a neutrinoless double beta decay rate accessible to upcoming searches, while  $\theta_{13} = 0$  giving no CP violation in neutrino oscillations. Note however that the connection of dark matter to neutrino properties depends strongly on how the symmetry breaking sector couples to the leptons.

## VIII. ACKNOWLEDGMENTS

This work was supported by the Spanish MICINN under grants FPA2008-00319/FPA and MULTIDARK Consolider CSD2009-00064, by Prometeo/2009/091, by the EU grant UNILHC PITN-GA-2009-237920. S. M. is supported by a Juan de la Cierva contract. E. P. is supported by CONACyT (Mexico).

### Appendix A: The $A_4$ group

All finite groups are completely characterized by means of a set of elements called generators of the group and a set of relations, so that all the elements of the group are given as product of the generators. The group  $A_4$  consists of the even permutations of four objects and then contains  $4!/2 = 12$  elements. The generators are  $S$  and  $T$  with the relations  $S^2 = T^3 = (ST)^3 = \mathcal{I}$ , then the elements are  $1, S, T, ST, TS, T^2, ST^2, STS, TST, T^2S, TST^2, T^2ST$ .

	$C_1 = \{I\}$	$C_2 = \{T\}$	$C_3 = \{T^2\}$	$C_4 = \{S\}$
1	1	1	1	1
1'	1	$\omega$	$\omega^2$	1
1''	1	$\omega^2$	$\omega$	1
3	3	0	0	-1

TABLE II: Character table of  $A_4$  where  $C_i$  are the different classes and  $\omega^3 \equiv 1$ .

$A_4$  has four irreducible representations (see Table II), three singlets 1, 1' and 1'' and one triplet. The one-dimensional unitary representations are obtained by:

$$\begin{aligned}
1 \quad S = 1 \quad T = 1 \\
1' \quad S = 1 \quad T = \omega \\
1'' \quad S = 1 \quad T = \omega^2
\end{aligned} \tag{A1}$$

where  $\omega^3 = 1$ . The product rule for the singlets are:

$$\begin{aligned}
1 \times 1 &= 1' \times 1'' = 1 \\
1' \times 1' &= 1'' \\
1'' \times 1'' &= 1'
\end{aligned} \tag{A2}$$

In the basis where  $S$  is real diagonal,

$$S = \begin{pmatrix} 1 & 0 & 0 \\ 0 & -1 & 0 \\ 0 & 0 & -1 \end{pmatrix}; \quad T = \begin{pmatrix} 0 & 1 & 0 \\ 0 & 0 & 1 \\ 1 & 0 & 0 \end{pmatrix}; \tag{A3}$$

one has the following triplet multiplication rules,

$$\begin{aligned}
(ab)_1 &= a_1 b_1 + a_2 b_2 + a_3 b_3; \\
(ab)_{1'} &= a_1 b_1 + \omega a_2 b_2 + \omega^2 a_3 b_3; \\
(ab)_{1''} &= a_1 b_1 + \omega^2 a_2 b_2 + \omega a_3 b_3; \\
(ab)_{3_1} &= (a_2 b_3, a_3 b_1, a_1 b_2); \\
(ab)_{3_2} &= (a_3 b_2, a_1 b_3, a_2 b_1),
\end{aligned} \tag{A4}$$

where  $a = (a_1, a_2, a_3)$  and  $b = (b_1, b_2, b_3)$ .

### Appendix B: $SU(5)$ embedding of the model

In [9] the quark sector has not been studied and it is assumed that quarks are generically singlets of  $A_4$  in order to not couple to the DM. It is possible to extend such a model to the quarks by embedding it into the grand unified group  $SU(5)$ . It is beyond our scope to give a complete gran-unified model and we only sketch a simple way to embed the model presented in [9] into a grand unified group. The matter assignment is the following

	$T_1$	$T_2$	$T_3$	$F_1$	$F_2$	$F_3$	$N_T$	$N_4$
SU(5)	10	10	10	$\bar{5}$	$\bar{5}$	$\bar{5}$	1	1
$A_4$	1	1'	1''	1	1''	1'	3	1

where we have assumed three copies of ten-multiplets and three of five-multiplets of  $SU(5)$  to describe the three flavours. The scalar assignment is

SU(5)	$5_H$	$\bar{5}_H$	$5_\eta$	$45_H$
$A_4$	1	1	3	1

then the Lagrangian is given by

$$\mathcal{L}_{down} = y_1^{l,d} T_1 F_1 \bar{5}_H + y_2^{l,d} T_2 F_2 \bar{5}_H + y_3^{l,d} T_3 F_3 \bar{5}_H + y_1^{l,d} T_1 F_1 45_H + y_2^{l,d} T_2 F_2 45_H + y_3^{l,d} T_3 F_3 45_H; \quad (\text{B1})$$

$$\mathcal{L}_{up} = y_1^u T_1 T_1 5_H + y_2^u T_2 T_3 5_H + y_1^u T_1 T_1 45_H + y_2^u T_2 T_3 45_H; \quad (\text{B2})$$

$$\mathcal{L}_\nu = y_1^\nu T_1 N_4 5_H + y_2^\nu T_2 N_4 5_H + y_3^\nu T_3 N_4 5_H + y_1^\nu T_1 N_T 5_\eta + M_1 N_T N_T + M_2 N_4 N_4. \quad (\text{B3})$$

The charged lepton and down quark mass matrix are diagonal with eigenvalues

$$m_e = y_1^{l,d} \langle 5_H \rangle - 3y_1^{l,d} \langle 45_H \rangle; \quad m_\mu = y_2^{l,d} \langle 5_H \rangle - 3y_2^{l,d} \langle 45_H \rangle; \quad m_\tau = y_3^{l,d} \langle 5_H \rangle - 3y_3^{l,d} \langle 45_H \rangle; \quad (\text{B4})$$

$$m_d = y_1^{l,d} \langle 5_H \rangle + y_1^{l,d} \langle 45_H \rangle; \quad m_s = y_2^{l,d} \langle 5_H \rangle + y_2^{l,d} \langle 45_H \rangle; \quad m_b = y_3^{l,d} \langle 5_H \rangle + y_3^{l,d} \langle 45_H \rangle;$$

and the three charged lepton masses as well as the three down quark masses can be easily reproduced. The up quark mass matrix is

$$M^u = \begin{pmatrix} m_u & 0 & 0 \\ 0 & 0 & m_c \\ 0 & m_t & 0 \end{pmatrix}, \quad M^u M^{u\dagger} = \begin{pmatrix} m_u^2 & 0 & 0 \\ 0 & m_c^2 & 0 \\ 0 & 0 & m_t^2 \end{pmatrix}, \quad (\text{B5})$$

where

$$m_u = y_1^u \langle 5_H \rangle; \quad m_c = y_2^u \langle 5_H \rangle - y_2^u \langle 45_H \rangle; \quad m_t = y_2^u \langle 5_H \rangle + y_2^u \langle 45_H \rangle. \quad (\text{B6})$$

Given the structure of the up and down quark mass matrices, the quark mixing matrix is diagonal. While this may be regarded as a good first approximation, since quark mixing angles are small, clearly another ingredient is needed such as, possibly, radiative corrections or extra vectorlike quark states. A full fit of the quark sector observables within a unified extension incorporating the flavour symmetry is beyond the scope of our paper.

### Appendix C: Mass spectrum

To simplify the notation we define the following combinations of couplings:

$$L = \lambda_9 + \lambda_{10} + 2\lambda_{11}, \quad (\text{C1})$$

$$Q = \lambda_{12} + \lambda_{13} + \lambda_{14} + \lambda_{15}, \quad (\text{C2})$$

$$P = \lambda_2 + \lambda_3 + 2\lambda_4 + \lambda_5, \quad (\text{C3})$$

$$R_1 = (-3\lambda_3 - 6\lambda_4 + 2\lambda_6 + \lambda_7 + \lambda_8), \quad (\text{C4})$$

$$R_2 = (-3\lambda_3 - 2\lambda_4 - 2\lambda_6 + \lambda_7 + \lambda_8 - 4\lambda_5), \quad (\text{C5})$$

$$R_3 = (-3\lambda_3 - 4\lambda_4 - 2\lambda_5 + \lambda_8). \quad (\text{C6})$$

The neutral scalars mass-matrix in the basis  $H'_0 - H'_1 - A'_0 - A'_1 - H'_2 - H'_3 - A'_2 - A'_3$  is block diagonal because of the  $Z_2$  symmetry and CP-conservation. It is given by:

$$M_{neutrals} = \begin{pmatrix} M_{HH_0} & 0 & 0 & 0 \\ 0 & M_{GA_0} & 0 & 0 \\ 0 & 0 & M_{H_2H_3} & 0 \\ 0 & 0 & 0 & M_{A_2A_3} \end{pmatrix}, \quad (\text{C7})$$

and the charged scalars mass matrix in the basis  $H_0'^+ - H_1'^+ - H_2'^+ - H_3'^+$  is:

$$M_{charged} = \begin{pmatrix} M_{G^+H_0^+} & 0 \\ 0 & M_{H_2^+H_3^+} \end{pmatrix}. \quad (C8)$$

The matrices  $M_{GA_0}$  and  $M_{G^+H_0^+}$  have a vanishing eigenvalue corresponding respectively to the neutral and charged Goldstone bosons eaten up by the  $Z$  and  $W^\pm$  gauge bosons. The diagonalization of the mass matrices goes as follows:

$$\begin{aligned} D_{HH_0} &= U_{HH_0}^\dagger M_{HH_0} U_{HH_0}; & D_{GA_0} &= U_{GA_0}^\dagger M_{GA_0} U_{GA_0}; \\ D_{G^+H_0^+} &= U_{G^+H_0^+}^\dagger M_{G^+H_0^+} U_{G^+H_0^+}; & M_{X_2X_3} &= U_{23}^\dagger M_{X_2X_3} U_{23}, \end{aligned} \quad (C9)$$

with  $X = H, A, H^+$  and

$$U_{GA_0} = U_{G^+H_0^+} = \begin{pmatrix} \cos \beta & -\sin \beta \\ \sin \beta & \cos \beta \end{pmatrix}; \quad U_{23} = \begin{pmatrix} -1/\sqrt{2} & 1/\sqrt{2} \\ 1/\sqrt{2} & 1/\sqrt{2} \end{pmatrix}; \quad (C10)$$

The mixing angle between  $\eta_2$  and  $\eta_3$  is  $\pi/4$ . The ratio of the vevs was parametrized by the angle  $\beta$  that controls the mixing within the  $Z_2$ -even sector for the charged scalars and pseudoscalars:

$$\begin{aligned} v^2 &= v_\eta^2 + v_H^2; \\ \tan \beta &= v_H/v_\eta. \end{aligned} \quad (C11)$$

We do not report the lengthy expression for  $U_{HH_0}$ . The mass spectrum reads then as:

$$M_{A_0}^2 = -2v^2\lambda_{11}, \quad (C12)$$

$$M_H^2 = \lambda_1 v_H^2 + P v_\eta^2 - \sqrt{(v_\eta^2 v_H^2 (L^2 - 4P\lambda_1) + (P v_\eta^2 + \lambda_1 v_H^2)^2)}, \quad (C13)$$

$$M_{H_0}^2 = \lambda_1 v_H^2 + P v_\eta^2 + \sqrt{(v_\eta^2 v_H^2 (L^2 - 4P\lambda_1) + (P v_\eta^2 + \lambda_1 v_H^2)^2)}, \quad (C14)$$

$$M_{H_0^+}^2 = -(\lambda_{10} + 2\lambda_{11})v^2/2, \quad (C15)$$

$$M_{H_2}^2 = v_\eta(-3Qv_H + R_1v_\eta)/2, \quad (C16)$$

$$M_{A_2}^2 = (-4\lambda_{11}v_H^2 + Qv_\eta v_H + R_2v_\eta^2)/2, \quad (C17)$$

$$M_{H_2^+}^2 = (v_H^2(\lambda_{10} + 2\lambda_{11}) - Qv_\eta v_H + R_3v_\eta^2)/2, \quad (C18)$$

$$M_{H_3}^2 = M_{H_2}^2 + 3Qv_H v_\eta, \quad (C19)$$

$$M_{A_3}^2 = M_{A_2}^2 + Qv_H v_\eta, \quad (C20)$$

$$M_{H_3^+}^2 = M_{H_2^+}^2 + Qv_H v_\eta. \quad (C21)$$

#### Appendix D: Oblique parameters

Following the notation of [28], the  $T$  oblique parameter for the standard model extended by  $n$  higgs doublets with hypercharge 1/2 is :

$$\Delta\rho = \alpha T = \frac{g^2}{64\pi^2 m_W^2} \left\{ \sum_{a=2}^n \sum_{b=2}^{2n} |(U^\dagger V)_{ab}|^2 F(m_a^2, \mu_b^2) \right. \quad (D1)$$

$$\left. - \sum_{b=2}^{2n-1} \sum_{b'=b+1}^{2n} [\text{Im}(V^\dagger V)_{bb'}]^2 F(\mu_b^2, \mu_{b'}^2) \right. \quad (D2)$$

$$\left. - 2 \sum_{a=2}^{n-1} \sum_{a'=a+1}^n |(U^\dagger U)_{aa'}|^2 F(m_a^2, m_{a'}^2) \right. \quad (D3)$$

$$\left. + 3 \sum_{b=2}^{2n} [\text{Im}(V^\dagger V)_{1b}]^2 [F(m_Z^2, \mu_b^2) - F(m_W^2, \mu_b^2)] \right. \quad (D4)$$

$$\left. - 3 [F(m_Z^2, m_h^2) - F(m_W^2, m_h^2)] \right\}, \quad (D5)$$

where  $m_a$ ,  $m_a$  denote the masses of the charged scalars and  $\mu_b$ ,  $\mu_b$  are the masses of the neutral ones,  $\alpha$  is the fine-structure constant and the function  $F$  is defined as ( $x, y > 0$ ):

$$F(x, y) \equiv \begin{cases} \frac{x+y}{2} - \frac{xy}{x-y} \ln \frac{x}{y} & \Leftarrow x \neq y, \\ 0 & \Leftarrow x = y. \end{cases} \quad (\text{D6})$$

We evaluate the  $U$  and  $V$  matrices for our model as:

$$U = \begin{pmatrix} U_{G^+H_0^+} & 0 \\ 0 & U_{23} \end{pmatrix}; \quad V = \begin{pmatrix} iU_{G^+H_0^+} & U_{HH_0} & 0 & 0 \\ 0 & 0 & U_{23} & iU_{23} \end{pmatrix}. \quad (\text{D7})$$

- 
- [1] G. Bertone, D. Hooper, and J. Silk, “Particle dark matter: Evidence, candidates and constraints,” *Phys.Rept.*, vol. 405, pp. 279–390, 2005.
- [2] M. Taoso, G. Bertone, and A. Masiero, “Dark Matter Candidates: A Ten-Point Test,” *JCAP*, vol. 0803, p. 022, 2008.
- [3] T. Hambye, “On the stability of particle dark matter,” [arXiv:1012.4587 [hep-ph]].
- [4] M. Frigerio and T. Hambye, “Dark matter stability and unification without supersymmetry,” *Phys. Rev.*, vol. D81, p. 075002, 2010.
- [5] M. Kadastik, K. Kannike, and M. Raidal, “Less-dimensions and matter parity as the origin of Dark Matter,” *Phys. Rev.*, vol. D81, p. 015002, 2010.
- [6] B. Batell, “Dark Discrete Gauge Symmetries,” [arXiv:1007.0045 [hep-ph]].
- [7] S. P. Martin, “Some simple criteria for gauged R-parity,” *Phys.Rev.*, vol. D46, pp. 2769–2772, 1992.
- [8] M. Cirelli, N. Fornengo, and A. Strumia, “Minimal dark matter,” *Nucl.Phys.*, vol. B753, pp. 178–194, 2006.
- [9] M. Hirsch, S. Morisi, E. Peinado, and J. W. F. Valle, “Discrete dark matter,” *Phys. Rev.*, vol. D82, p. 116003, 2010.
- [10] T. Schwetz, M. Tortola, and J. W. F. Valle, “Three-flavour neutrino oscillation update,” *New J. Phys.*, vol. 10, p. 113011, 2008.
- [11] Y. Kajiyama and H. Okada, “T(13) Flavor Symmetry and Decaying Dark Matter,” [arXiv:1011.5753 [hep-ph]].
- [12] V. Berezinsky and J. W. F. Valle, “The keV majoron as a dark matter particle,” *Phys. Lett.*, vol. B318, pp. 360–366, 1993.
- [13] M. Lattanzi and J. W. F. Valle, “Decaying warm dark matter and neutrino masses,” *Phys. Rev. Lett.*, vol. 99, p. 121301, 2007.
- [14] F. Bazzocchi, M. Lattanzi, S. Riemer-Sorensen, and J. W. F. Valle, “X-ray photons from late-decaying majoron dark matter,” *JCAP*, vol. 0808, p. 013, 2008.
- [15] P. Minkowski, “ $\mu \rightarrow e \gamma$  at a rate of one out of 1-billion muon decays?,” *Phys. Lett.*, vol. B67, p. 421, 1977.
- [16] M. Gell-Mann, P. Ramond, and R. Slansky, “Complex spinors and unified theories,” 1979. Print-80-0576 (CERN).
- [17] T. Yanagida, “Kek lectures,” KEK lectures, 1979. ed. Sawada and Sugamoto (KEK, 1979).
- [18] R. N. Mohapatra and G. Senjanovic, “Neutrino mass and spontaneous parity nonconservation,” *Phys. Rev. Lett.*, vol. 44, p. 91, 1980.
- [19] J. Schechter and J. W. F. Valle, “Neutrino masses in  $su(2) \times u(1)$  theories,” *Phys. Rev.*, vol. D22, p. 2227, 1980.
- [20] D. Meloni, S. Morisi, E. Peinado, “Neutrino phenomenology and stable dark matter with A4,” [arXiv:1011.1371 [hep-ph]].
- [21] K. Babu, E. Ma, and J. Valle, “Underlying A(4) symmetry for the neutrino mass matrix and the quark mixing matrix,” *Phys.Lett.*, vol. B552, pp. 207–213, 2003.
- [22] R. Bernabei *et al.*, “New results from DAMA/LIBRA,” *Eur. Phys. J.*, vol. C67, pp. 39–49, 2010.
- [23] R. Bernabei *et al.*, “Search for WIMP annual modulation signature: Results from DAMA / NaI-3 and DAMA / NaI-4 and the global combined analysis,” *Phys. Lett.*, vol. B480, pp. 23–31, 2000.
- [24] C. E. Aalseth *et al.*, “Results from a Search for Light-Mass Dark Matter with a P- type Point Contact Germanium Detector,” [arXiv:1002.4703 [astro-ph.CO]].
- [25] M. E. Peskin and T. Takeuchi, “Estimation of oblique electroweak corrections,” *Phys. Rev.*, vol. D46, pp. 381–409, 1992.
- [26] W. Grimus, L. Lavoura, O. M. Ogreid, and P. Osland, “The oblique parameters in multi-Higgs-doublet models,” *Nucl. Phys.*, vol. B801, pp. 81–96, 2008.

- [27] R. Barbieri, L. J. Hall, and V. S. Rychkov, “Improved naturalness with a heavy Higgs: An alternative road to LHC physics,” *Phys. Rev.*, vol. D74, p. 015007, 2006.
- [28] W. Grimus, L. Lavoura, O. Ogreid, and P. Osland, “A Precision constraint on multi-Higgs-doublet models,” *J.Phys.G*, vol. G35, p. 075001, 2008.
- [29] K. Nakamura *et al.*, “Review of particle physics,” *J. Phys.*, vol. G37, p. 075021, 2010.
- [30] A. Pierce and J. Thaler, “Natural Dark Matter from an Unnatural Higgs Boson and New Colored Particles at the TeV Scale,” *JHEP*, vol. 0708, p. 026, 2007.
- [31] E. Lundstrom, M. Gustafsson, and J. Edsjo, “The Inert Doublet Model and LEP II Limits,” *Phys. Rev.*, vol. D79, p. 035013, 2009.
- [32] G. Belanger, F. Boudjema, P. Brun *et al.*, “Indirect search for dark matter with micrOMEGAs2.4,” [arXiv:1004.1092 [hep-ph]].
- [33] G. Belanger, F. Boudjema, A. Pukhov, and A. Semenov, “Dark matter direct detection rate in a generic model with micrOMEGAs2.1,” *Comput. Phys. Commun.*, vol. 180, pp. 747–767, 2009.
- [34] L. Lopez-Honorez and C. E. Yaguna, “A new viable region of the inert doublet model,” [arXiv:1011.1411 [hep-ph]].
- [35] L. Lopez Honorez, C. E. Yaguna, “The inert doublet model of dark matter revisited,” *JHEP* **1009** (2010) 046. [arXiv:1003.3125 [hep-ph]].
- [36] N. Fornengo, S. Scopel, and A. Bottino, “Discussing direct search of dark matter particles in the Minimal Supersymmetric extension of the Standard Model with light neutralinos,” [arXiv:1011.4743 [hep-ph]].
- [37] C. Savage, G. Gelmini, P. Gondolo, and K. Freese, “XENON10/100 dark matter constraints in comparison with CoGeNT and DAMA: examining the  $\text{Leff}$  dependence,” [arXiv:1006.0972 [astro-ph.CO]].
- [38] Z. Ahmed *et al.*, “Dark Matter Search Results from the CDMS II Experiment,” *Science*, vol. 327, pp. 1619–1621, 2010.
- [39] Z. Ahmed *et al.*, “Results from a Low-Energy Analysis of the CDMS II Germanium Data,” *Phys.Rev.Lett.*, 2010.
- [40] E. Aprile *et al.*, “First Dark Matter Results from the XENON100 Experiment,” *Phys.Rev.Lett.*, vol. 105, p. 131302, 2010.
- [41] A. Abdo, M. Ackermann, M. Ajello, W. Atwood, L. Baldini, *et al.*, “Observations of Milky Way Dwarf Spheroidal galaxies with the Fermi-LAT detector and constraints on Dark Matter models,” *Astrophys.J.*, vol. 712, pp. 147–158, 2010.
- [42] A. Abdo *et al.*, “Constraints on Cosmological Dark Matter Annihilation from the Fermi-LAT Isotropic Diffuse Gamma-Ray Measurement,” *JCAP*, vol. 1004, p. 014, 2010.
- [43] K. N. Abazajian, S. Blanchet, and J. P. Harding, “Enhanced Dark Matter Sensitivity from Fermi-LAT Resolution of the Diffuse Gamma-Ray Background,” [arXiv:1011.5090 [hep-ph]].
- [44] J. Kopp, T. Schwetz, and J. Zupan, “Global interpretation of direct Dark Matter searches after CDMS-II results,” *JCAP*, vol. 1002, p. 014, 2010.
- [45] S. Andreas, C. Arina, T. Hambye, F.-S. Ling, and M. H. Tytgat, “A light scalar WIMP through the Higgs portal and CoGeNT,” *Phys.Rev.*, vol. D82, p. 043522, 2010.
- [46] P. Belli, R. Bernabei, A. Bottino, F. Donato, N. Fornengo, *et al.*, “Extending the DAMA annual modulation region by inclusion of the uncertainties in the astrophysical velocities,” *Phys.Rev.*, vol. D61, p. 023512, 2000.
- [47] A. M. Green, “Dependence of direct detection signals on the WIMP velocity distribution,” *JCAP* **1010** (2010) 034.
- [48] P. J. Fox, J. Liu, and N. Weiner, “Integrating Out Astrophysical Uncertainties,” [arXiv:1011.1915 [hep-ph]].
- [49] N. Bozorgnia, G. B. Gelmini, and P. Gondolo, “Channeling in direct dark matter detection V: channeling fraction in solid Xe, Ar and Ne,” [arXiv:1011.6006 [astro-ph.CO]].
- [50] V. Barger, W.-Y. Keung, and D. Marfatia, “Electromagnetic properties of dark matter: dipole moments and charge form factor,” *Phys. Lett.* **B696** (2011) 74-78.
- [51] D. Tucker-Smith and N. Weiner, “Inelastic dark matter,” *Phys. Rev.*, vol. D64, p. 043502, 2001.
- [52] S. Chang, A. Pierce, and N. Weiner, “Momentum Dependent Dark Matter Scattering,” *JCAP*, vol. 1001, p. 006, 2010.
- [53] W. Seidel, “Talk on behalf of the cress collaboration at idm montpellier.” 2010.
- [54] T. Schwetz, “Direct detection data and possible hints for low-mass WIMPs,” [arXiv:1011.5432 [hep-ph]].
- [55] J. Collar, “Light WIMP Searches: The Effect of the Uncertainty in Recoil Energy Scale and Quenching Factor,” [arXiv:1010.5187 [astro-ph.IM]].
- [56] M. Ibe, H. Murayama, and T. Yanagida, “Breit-Wigner Enhancement of Dark Matter Annihilation,” *Phys.Rev.*, vol. D79, p. 095009, 2009.
- [57] W.-L. Guo and Y.-L. Wu, “Enhancement of Dark Matter Annihilation via Breit-Wigner Resonance,” *Phys.Rev.*, vol. D79, p. 055012, 2009.
- [58] D. Feldman, Z. Liu, and P. Nath, “PAMELA Positron Excess as a Signal from the Hidden Sector,” *Phys.Rev.*, vol. D79, p. 063509, 2009.
- [59] M. Ibe, Y. Nakayama, H. Murayama, and T. T. Yanagida, “Nambu-Goldstone Dark Matter and Cosmic Ray Electron and

- Positron Excess,” *JHEP*, vol. 0904, p. 087, 2009.
- [60] M. Ackermann, M. Ajello, A. Allafort, L. Baldini, J. Ballet, *et al.*, “Constraints on Dark Matter Annihilation in Clusters of Galaxies with the Fermi Large Area Telescope,” *JCAP*, vol. 1005, p. 025, 2010.
- [61] M. Papucci and A. Strumia, “Robust implications on Dark Matter from the first FERMI sky gamma map,” *JCAP*, vol. 1003, p. 014, 2010.
- [62] M. Cirelli, P. Panci, and P. D. Serpico, “Diffuse gamma ray constraints on annihilating or decaying Dark Matter after Fermi,” *Nucl. Phys.*, vol. B840, pp. 284–303, 2010.
- [63] G. Zaharijas, A. Cuoco, Z. Yang, and J. Conrad, “Constraints on the Galactic Halo Dark Matter from Fermi- LAT Diffuse Measurements,” [arXiv:1012.0588 [astro-ph.HE]].
- [64] B. Anderson, “Fermi-LAT constraints on diffuse Dark Matter annihilation from the Galactic Halo,” [arXiv:1012.0863 [hep-ph]].
- [65] A. Cuoco, A. Sellerholm, J. Conrad, and S. Hannestad, “Anisotropies in the Diffuse Gamma-Ray Background from Dark Matter with Fermi LAT: a closer look,” [arXiv:1005.0843 [astro-ph.HE]].